Research Article | Vol. 25, No. 26 | 25 Dec 2017 | OPTICS EXPRESS 33688
Optics EXPRESS

Polarization-independent phase modulators enabled by two-photon polymerization

ZIQIAN HE,[1] YUN-HAN LEE,[1] FANGWANG GOU,[1] DANIEL FRANKLIN,[2,3] DEBASHIS CHANDA,[1,2,3,4] AND SHIN-TSON WU[1,*]

[1]*College of Optics and Photonics, University of Central Florida, Orlando, 32816, USA*
[2]*Department of Physics, University of Central Florida, 32816, USA*
[3]*NanoScience Technology Center, University of Central Florida Orlando, 32826, USA*
[4]*Debashis.Chanda@creol.ucf.edu*
**swu@creol.ucf.edu*

Abstract: A double-layer polarization-independent liquid crystal (LC) phase modulator is demonstrated and characterized. Using two-photon polymerization process, an ultra-thin partition polymeric film to separate the LC cell into two layers with orthogonal alignment directions is fabricated. Such a thin partition film also helps to reduce the voltage shielding effect. Using a high birefringence and low viscosity LC mixture, 2π phase change at merely 10 V for a He-Ne laser beam is achieved, while keeping a fast response time. Simulation result agrees reasonably well with experimental data.

OCIS codes: (160.3710) Liquid crystals; (260.5430) Polarization; (060.5060) Phase modulation; (220.4241) Nanostructure fabrication; (050.6875) Three-dimensional fabrication.

References and links

1. H. Sasaki, K. Yamamoto, Y. Ichihashi, and T. Senoh, "Image size scalable full-parallax coloured three-dimensional video by electronic holography," Sci. Rep. **4**(1), 4000 (2014).
2. A. M. Weiner, "Femtosecond pulse shaping using spatial light modulators," Rev. Sci. Instrum. **71**(5), 1929–1960 (2000).
3. J. Wang, J.-Y. Yang, I. M. Fazal, N. Ahmed, Y. Yan, H. Huang, Y. Ren, Y. Yue, S. Dolinar, M. Tur, and A. E. Willner, "Terabit free-space data transmission employing orbital angular momentum multiplexing," Nat. Photonics **6**(7), 488–496 (2012).
4. N. Bozinovic, Y. Yue, Y. Ren, M. Tur, P. Kristensen, H. Huang, A. E. Willner, and S. Ramachandran, "Terabit-Scale Orbital Angular Momentum Mode Division Multiplexing in Fibers," Science **340**(6140), 1545–1548 (2013).
5. R. A. Forber, A. Au, U. Efron, K. Sayyah, S.-T. Wu, and G. C. Goldsmith II, "Dynamic IR scene projection using the Hughes liquid crystal light valve," Proc. SPIE **1665**, 259–273 (1992).
6. P. F. McManamon, T. A. Dorschner, D. L. Corkum, L. J. Friedman, D. S. Hobbs, M. Holz, S. Liberman, H. Q. Nguyen, D. P. Resler, R. C. Sharp, and E. A. Watson, "Optical Phased Array Technology," Proc. IEEE **84**(2), 268–298 (1996).
7. F. Peng, Y.-H. Lee, H. Chen, Z. Li, A. E. Bostwick, R. J. Twieg, and S.-T. Wu, "Low absorption chlorinated liquid crystals for infrared applications," Opt. Mater. Express **5**(6), 1281–1288 (2015).
8. H. Ren and S.-T. Wu, *Introduction to Adaptive Lenses* (John Wiley & Sons, Inc., 2012).
9. M. P. J. Lavery, F. C. Speirits, S. M. Barnett, and M. J. Padgett, "Detection of a spinning object using light's orbital angular momentum," Science **341**(6145), 537–540 (2013).
10. H. Kikuchi, M. Yokota, Y. Hisakado, H. Yang, and T. Kajiyama, "Polymer-stabilized liquid crystal blue phases," Nat. Mater. **1**(1), 64–68 (2002).
11. R. M. Hyman, A. Lorenz, S. M. Morris, and T. D. Wilkinson, "Polarization-independent phase modulation using a blue-phase liquid crystal over silicon device," Appl. Opt. **53**(29), 6925–6929 (2014).
12. F. Peng, Y.-H. Lee, Z. Luo, and S.-T. Wu, "Low voltage blue phase liquid crystal for spatial light modulators," Opt. Lett. **40**(21), 5097–5100 (2015).
13. M. J. Sansone, G. Khanarian, T. M. Leslie, M. Stiller, J. Altman, and P. Elizondo, "Large Kerr effects in transparent encapsulated liquid crystals," J. Appl. Phys. **67**(9), 4253–4259 (1990).
14. D. E. Lucchetta, R. Karapinar, A. Manni, and F. Simoni, "Phase-only modulation by nanosized polymer-dispersed liquid crystals," J. Appl. Phys. **91**(9), 6060–6065 (2002).
15. H. Ren, Y.-H. Lin, Y.-H. Fan, and S.-T. Wu, "Polarization-independent phase modulation using a polymer-dispersed liquid crystal," Appl. Phys. Lett. **86**(14), 141110 (2005).
16. H. Ren, Y.-H. Lin, C.-H. Wen, and S.-T. Wu, "Polarization-independent phase modulation of a homeotropic liquid crystal gel," Appl. Phys. Lett. **87**(19), 191106 (2005).

#313306 https://doi.org/10.1364/OE.25.033688
Journal © 2017 Received 13 Nov 2017; revised 14 Dec 2017; accepted 21 Dec 2017; published 22 Dec 2017

Optics EXPRESS

17. Y. Huang, C.-H. Wen, and S.-T. Wu, "Polarization-independent and submillisecond response phase modulators using a 90° twisted dual-frequency liquid crystal," Appl. Phys. Lett. **89**(2), 021103 (2006).
18. H. Ren, Y.-H. Lin, and S.-T. Wu, "Polarization-independent and fast-response phase modulators using double-layered liquid crystal gels," Appl. Phys. Lett. **88**(6), 061123 (2006).
19. J. S. Patel, "Polarization insensitive tunable liquid-crystal etalon filter," Appl. Phys. Lett. **59**(11), 1314–1316 (1991).
20. M. Choi and J. Choi, "Universal phase-only spatial light modulators," Opt. Express **25**(19), 22253–22267 (2017).
21. Y.-H. Lin, H. Ren, Y.-H. Wu, Y. Zhao, J. Fang, Z. Ge, and S.-T. Wu, "Polarization-independent liquid crystal phase modulator using a thin polymer-separated double-layered structure," Opt. Express **13**(22), 8746–8752 (2005).
22. Y.-H. Lin, M.-S. Chen, W.-C. Lin, and Y.-S. Tsou, "A polarization-independent liquid crystal phase modulation using polymer-network liquid crystals in a 90 degree twisted cell," J. Appl. Phys. **112**(2), 024505 (2012).
23. S.-T. Wu, "Design of a liquid crystal based tunable electro-optic filter," Appl. Opt. **28**(1), 48–52 (1989).
24. B. H. Cumpston, S. P. Ananthavel, S. Barlow, D. L. Dyer, J. E. Ehrlich, L. L. Erskine, A. A. Heikal, S. M. Kuebler, I.-Y. S. Lee, D. McCord-Maughon, J. Qin, H. Röckel, M. Rumi, X. L. Wu, S. R. Marder, and J. W. Perry, "Two-photon polymerization initiators for three-dimensional optical data storage and microfabrication," Nature **398**(6722), 51–54 (1999).
25. J. Serbin, A. Egbert, A. Ostendorf, B. N. Chichkov, R. Houbertz, G. Domann, J. Schulz, C. Cronauer, L. Fröhlich, and M. Popall, "Femtosecond laser-induced two-photon polymerization of inorganic-organic hybrid materials for applications in photonics," Opt. Lett. **28**(5), 301–303 (2003).
26. Y.-H. Lee, D. Franklin, F. Gou, G. Liu, F. Peng, D. Chanda, and S.-T. Wu, "Two-photon polymerization enabled multi-layer liquid crystal phase modulator," Sci. Rep. **7**(1), 16260 (2017).
27. C.-H. Lee, H. Yoshida, Y. Miura, A. Fujii, and M. Ozaki, "Local liquid crystal alignment on patterned micrograting structures photofabricated by two photon excitation direct laser writing," Appl. Phys. Lett. **93**(17), 173509 (2008).
28. D. Karalekas and A. Aggelopoulos, "Study of shrinkage strains in a stereolithography cured acrylic photopolymer resin," J. Mater. Process. Technol. **136**(1–3), 146–150 (2003).
29. M. Schadt and W. Helfrich, "Voltage-dependent optical activity of a twisted nematic liquid crystal," Appl. Phys. Lett. **18**(4), 127–128 (1971).
30. D. Franklin, Y. Chen, A. Vazquez-Guardado, S. Modak, J. Boroumand, D. Xu, S.-T. Wu, and D. Chanda, "Polarization-independent actively tunable colour generation on imprinted plasmonic surfaces," Nat. Commun. **6**, 7337 (2015).

1. Introduction

Phase-only spatial light modulators (SLMs) are widely used in holograms [1], laser pulse shaping [2], optical communications [3,4], laser beam steering [5–7], tunable-focus lens [8], and optical angular momentum control [9]. Typically, to realize phase-only modulation, a linearly polarized light is required. For the above-mentioned applications, a polarization-independent SLM is highly desirable. Currently, three types of liquid-crystal (LC) polarization-independent phase modulators have been developed. The first is based on optically isotropic media, such as polymer-stabilized blue phase LC (BPLC) [10–12] and nanoscale polymer-dispersed LC (nano-PDLC) [13–15]. In the voltage-off state, the medium is optically isotropic, i.e. its refractive index is equal in all directions ($n = n_i$). In presence of longitudinal electric field (E) (say in the z-axis), the effective refractive index sphere stretches along that direction, forming an optical axis. As the voltage changes, light traversing through the optical axis will experience a different effective refractive index ($n_o(E)$). The advantages of such an isotropic-to-anisotropic transition are twofold: it is polarization independent, and its response time is fast (<1 ms). However, two challenges remain to be overcome before these Kerr media can find practical applications: 1) the required operation voltage is relatively high (>50 V; depending on the dielectric anisotropy of the employed LC), and 2) the effective refractive index change (n_i-n_o) is only one-third of the LC birefringence ($\Delta n = n_e$-n_o).

The second approach is called residual phase change [16–18]. For instance, the phase of a 90° twisted nematic (TN) LC cell is polarization insensitive when the applied voltage is 3x greater than the threshold voltage [19]. While the bulk of the LC is aligned vertically along the applied field, the planar tilt of the LC near the anchoring surface imparts a phase change. Fast response time can be achieved in these devices, but the major tradeoff is its relatively small remaining phase change (<1π).

Optics EXPRESS

The third approach is to use multiple birefringent layers which can compensate for each other's phase [20–22]. A simple example is to stack two homogeneous LC layers with orthogonal alignment directions. In such a device, an effective refractive index ellipsoid is formed with the optical axis along stacking direction. This way, a phase change can be obtained by varying an electric field along the optical axis [21]. The merit of this approach is that an adequate phase change can be readily obtained. However, the major shortcoming is that the partition layer may shield the applied voltage significantly, depending on its thickness. From practical application viewpoint, a polarization-independent phase modulator should exhibit a minimum 2π phase change, fast response time, and low operation voltage (<15 V). The maximum phase change (δ) of a transmissive polarization-independent mode is determined by the effective birefringence (Δn_{eff}), cell gap (d) and wavelength (λ) as:

$$\delta = 2\pi d\Delta n_{eff} / \lambda. \quad (1)$$

Meanwhile, the response time is governed by the rotational viscosity (γ_1) and splay elastic constant (K_{11}) of the employed LC as [23]:

$$\tau = \frac{\gamma_1}{K_{11}}\frac{d^2}{\pi^2}. \quad (2)$$

From Eqs. (1) and (2), a larger cell gap produces more phase change, but the tradeoff is slower response time. A polarization-independent, fast response and low operating voltage (< 15 V) phase modulator with 2π phase change will add significant technological value.

In this paper, a double-layer polarization-independent phase modulator enabled by two-photon polymerization (TPP) [24,25] is demonstrated. In recent years, TPP has been widely applied to generate three-dimensional structure with sub-micron resolution. Here, by utilizing this technique, a suspended ultra-thin polymer film is fabricated to separate the two LC layers between glass substrates, while generating orthogonal alignment directions for the top and bottom layers. Polymeric pillars are included to precisely control the cell gap and ensure both LC layers have the same thickness. In this double-layer structure, response time is not determined by the total cell gap, but by the individual layer thickness. Ideally, by introducing this partition layer the response time should be 4x faster than that of conventional LC cell [26]. Simulation is performed to predict the device voltage-phase response while taking into consideration the voltage-shielding effect of the partition film. The simulation is verified through experiment, where a 3.3 by 3.3 mm^2 sample is fabricated and characterized. With the recently developed TPP process, the polarization-independent device exhibits a 2π phase change (λ = 633 nm) at 10 V with 8.85-ms relaxation time. This approach successfully eliminates the shortfalls of the aforementioned approaches and enables polarization-independent phase modulators for practical applications.

2. Results and discussion

Figure 1(a) schematically shows the device architecture. To fabricate the proposed double-layer structure, first the nano-groove alignment layer on the bottom glass substrate is patterned [27]. Next, arrays of pillars to serve as supports for the partition layer are formed which is followed by polymerization of the partition layer written with orthogonal directions on either side. At the end of the TPP process, four quadrants of pillar arrays slightly outside of the functional area are added to control the total cell gap to approximately 5.75 μm (details in the Methods section).

Figures 1(b)-1(d) show the scanning electron microscopy (SEM) images of a sample with dimension of 360 by 360 μm^2 before filling the LC. The distance between pillars within the functional area is 13 μm and the size of each pillar is 1.8 by 1.8 μm^2. The surrounding pillars are elongated to withstand the relaxation of the polymer film during TPP process [28]. Individual writing sections are 90 by 90 μm^2. Connecting bars are made to provide structural

Optics EXPRESS

stability over the large-area pattern and periodic holes are designed to help with development and evaporation of solvents in order to prevent structural collapse. The size of surrounding pillars and connecting bars is set to be 3 by 9 μm^2. Figure 1(d) demonstrates the function of the partition layer and shows the orthogonal alignment directions on the top and bottom sides of the partition, as indicated by the direction of the grooves. From SEM images the thickness of the bottom alignment layer and the partition layer are measured to be 0.1 μm and 1.4 μm, respectively. Subsequently, the thickness of each LC layer is estimated to be 2.12 μm from the total measured cell gap of 5.75 μm. It is noteworthy that, even though the partition layer is so thin, the structure is thermally stable as no noticeable changes are observed after heating the sample at 100 °C for two hours.

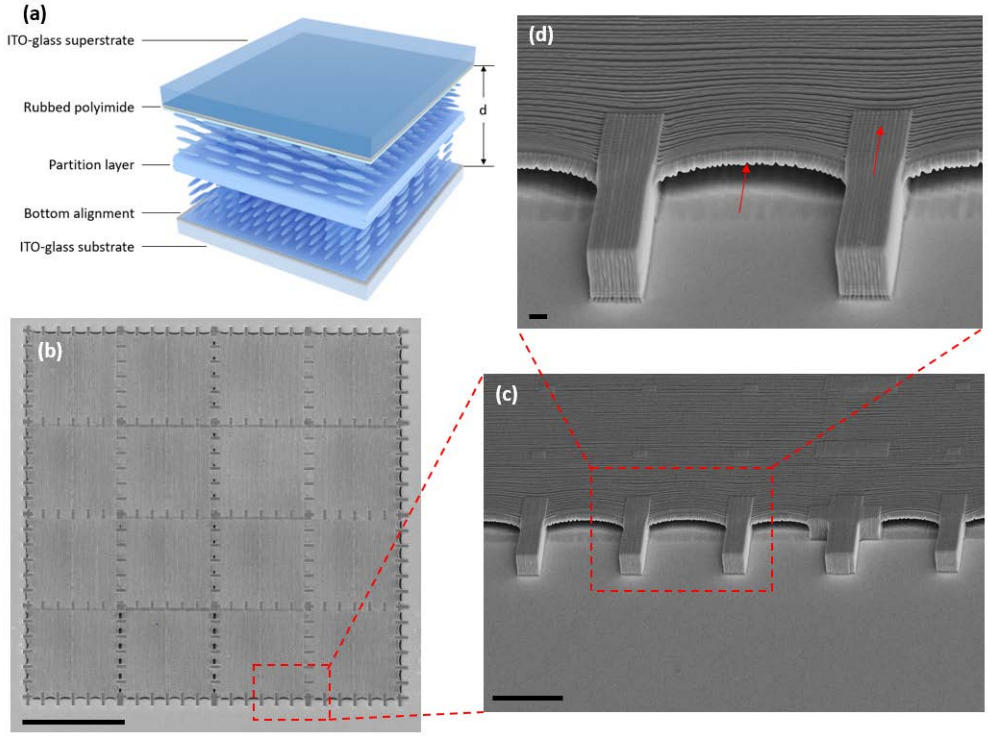

Fig. 1. (a) Schematic of the proposed structure, and (b-d) SEM images of a 360 by 360 μm^2 sample. The series illustrate more details of the structure. The red arrows in (d) denote that the alignment on the top of the pillars and under the partition layer is perpendicular to the alignment on the top of the partition layer. Scale bars: 100 μm (b), 10 μm (c), and 1 μm (d).

To investigate the scale-up capability, a 3.3 by 3.3 mm^2 sample is fabricated. Figure 2 shows the polarized optical microscope (POM) images of the sample where the polarizer and analyzer are crossed. In Figs. 2(a)-2(c), the bottom layer alignment of the sample is parallel, 45°, and perpendicular to the polarizer, respectively. The pillar arrays which control the total cell gap of the working area are shown in Fig. 2(d). It is worth noting that the bright spots in Figs. 2(a)-2(c) indicate the location of pillars and that they offer orthogonal alignment to that of the top layer, as shown in Fig. 1(d). The LC molecules between the pillar and the rubbed superstrate will rotate 90° along the stack direction, forming a twisted-nematic (TN) region. In the voltage-off state, a TN cell transmits light and appears white between crossed polarizers [29]. Also in Figs. 2(a) and 2(c), some dimmed but not dark spots are observed. These spots correspond to periodic holes which are designed to help with structure development, as mentioned before. The LC molecules above the holes have no preferential orientation, leading to light scattering in some extent. However, the light scattering

Optics EXPRESS

introduced by the holes is negligible as the size of the holes is small. Therefore, the actual working area is the dark area where nearly no light passing through the crossed polarizers. The aperture ratio of the fabricated structure is about 91%. By reducing the size of each pillar or further improving the stabilization structure, a larger working area is achievable. From Fig. 2(b), a small light leakage in some sites (dark blue color instead of black) is observed, indicating that the thickness of the two LC layers is not perfectly uniform across the entire working area. This non-uniformity could originate from the relaxation and lateral shrinkage of partition layer during polymerization process, therefore distorting the LC director.

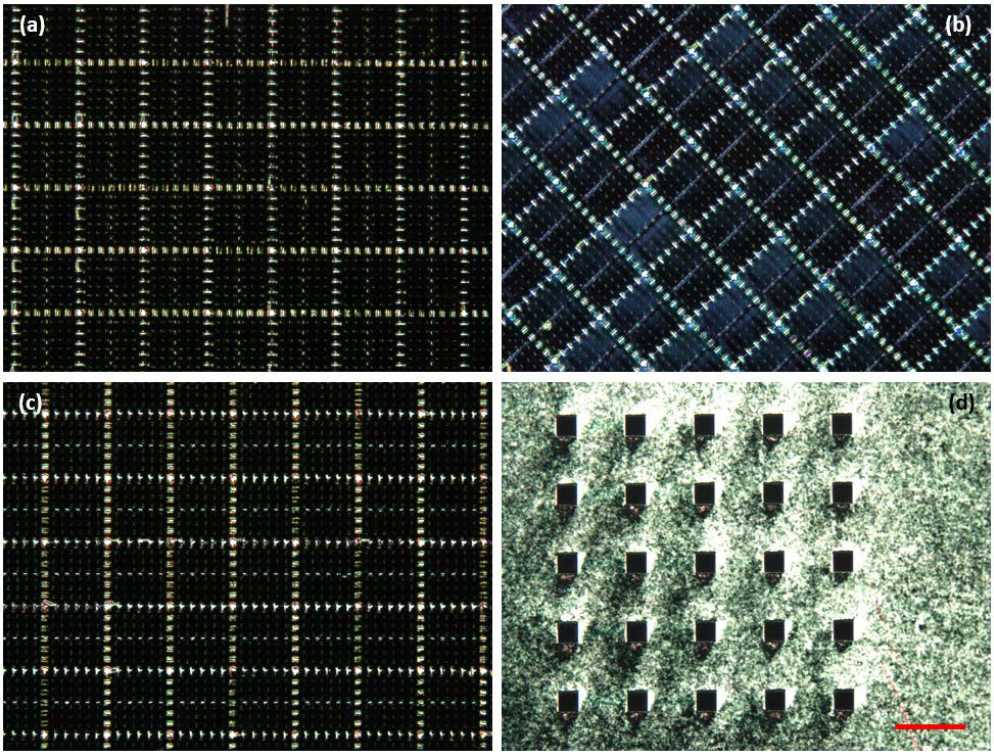

Fig. 2. POM images under crossed polarizers. Bottom layer alignment is (a) parallel, (b) 45°, (c) perpendicular to the polarizer. (d) Pillar arrays which control the total cell gap. Scale bar: 100 μm for all.

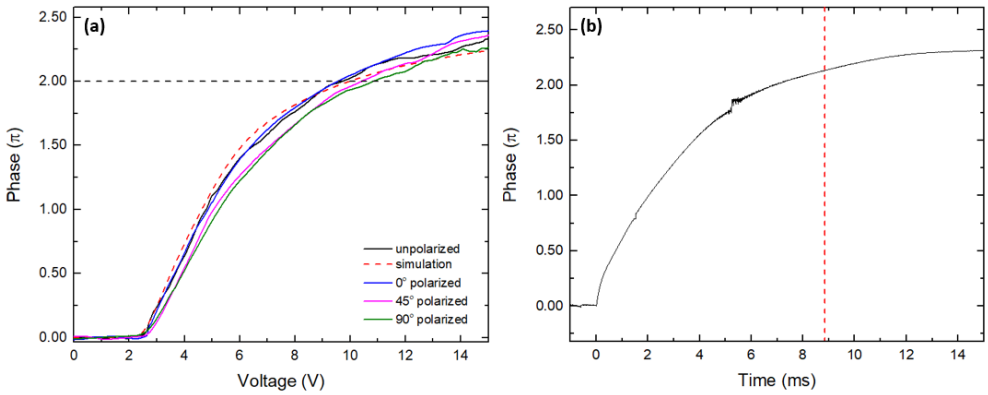

Fig. 3. (a) Simulated and measured voltage-phase responses of the two-layer LC cell under different input polarizations. Black dashed line denotes 2π phase change. (b) Measured

Optics EXPRESS

transient phase relaxation curve of the test cell where an unpolarized He-Ne laser beam is employed. Red dashed lines indicating the decay time (100% to 10%) is 8.85 ms at the room temperature (23°C).

To investigate the electro-optic response, the device is characterized with a Mach-Zehnder interferometer. The sample with 3.3-by-3.3 mm^2 working area is positioned at the center of one arm and a pinhole in front of the photodetector is used to select the region of the sample. By placing a linear polarizer after a unpolarized He-Ne laser (λ = 632.8 nm), input polarization is well controlled. Figure 3(a) shows the measured and simulated voltage-dependent phase change at different polarization states. The voltage-phase curves exhibit a small discrepancy for different polarizations, due to the slightly unequal thicknesses of the two LC layers. However, the overall response is polarization insensitive. Simulation result obtained by DIMOS software is shown by the red dashed curve which takes into account the voltage-shielding effect of polymer films. It agrees reasonably well with the experimental data. At 15 V, a phase change of 2.3 π is achieved at λ = 632.8 nm. The relaxation time (100% to 10%) of the phase modulator is measured using an unpolarized He-Ne laser beam to be 8.85 ms at 23°C as can be seen in Fig. 3(b).

The present cell in the transmissive mode provides a phase change of 1.2π at λ = 1.06 μm which can be doubled to 2.4π in reflection mode, while maintaining a fast 8.85 ms response time. In order to achieve the full 2π phase change, the thickness of each layer needs to be 3.6 μm and the response time increases by 2.88 times based on Eq. (2). The concept can be extended to longer wavelength range by either slightly increasing the cell gap or operating in reflective mode. Another solution of working at longer wavelength is to build more layers. The advantages include more total phase change and keeping fast response time, but the tradeoffs are linearly increased operation voltage and potential structure stability issue. In experiment, it is noticed that larger pillars are preferred to maintain the stability of the structure during the TPP process when more layers are required. This will also result in smaller working area as the pillars are enlarged.

3. Experimental methods

3.1 TPP processing

Polymer films and pillars were fabricated using a commercially available femtosecond laser lithography system (NanoScribe GmbH) [30]. Dip-in mode was used with a x63, 1.4 numerical aperture (NA) oil immersion objective (Zeiss) and IP-Dip (NanoScribe GmbH) photoresist. After dropping IP-Dip on a one-side ITO-coated glass substrate, the objective was directly immersed into the photoresist. A 2D galvanometer scanner was utilized to steer the focal point of a 780-nm pulsed laser to expose the photoresist line-by-line. Grooves with 300 nm periodicity were established, providing strong anchoring force to LC molecules. After the writing, the sample was gently immersed into 1,2-Propanediol monomethyl ether acetate (PGMEA) solution for 20 min to remove the unexposed photoresist, and then it was placed in isopropyl alcohol (IPA) for 5 min to remove PGMEA. Last, to evaporate the IPA, the sample was held at 20 cm above a 200 °C hot plate until all the droplets were completely evaporated.

3.2 LC cell finishing

A single-side ITO-coated glass superstrate with alignment perpendicular to that of the substrate was adhered to the structured substrate using NOA 81, together with some 4.5 μm silica spacers to share some pressure on polymerized pillars which maintain the total cell gap in the functional area. Once UV cured, the test cell was filled with a LC mixture LCM-1660 (LC Matter, USA) under 10 Torr environments. This LC material has a relatively high birefringence (Δn = 0.38 at λ = 632.8 nm, $\Delta\varepsilon$ = 16.01 at 1 kHz driving frequency, and γ_1/K_{11} = 16.59 ms/μm^2 at room temperature) so that a large phase change could be obtained.

Optics EXPRESS

3.3 Characterization

The morphology of the structure was investigated by SEM (Zeiss ULTRA-55 FEG SEM) at an accelerating voltage of 3.5 kV. The voltage-phase and time-phase responses were measured by a homemade Mach-Zehnder interferometer. The test cell was driven with 1 kHz AC sine wave to reduce ion migration. All the reported voltages are root mean square values.

3.4 DIMOS simulation

The simulation was conducted using commercial DIMOS software. It uses finite element method (FEM) to calculate the LC director distribution first. Then, either extended 2 by 2 Jones matrix or 4 by 4 Berreman matrix method is adopted to compute the optical response of the imported configuration.

4. Conclusion

A polarization-independent phase modulator enabled by the TPP process is designed and fabricated. A 2π phase change at 632.8 nm is achieved at 10 V with a relaxation time of 8.85 ms. Comparing to previous work, this design leads to a good compromise between phase change, operating voltage and relaxation time, which enhances the potential of this kind of phase modulator for practical applications. This strategy of using TPP for alignment and partition layer fabrication is promising in general three-dimensional configuration of LC and alignment of other materials like quantum rods.

Funding

Prof. Wu's group is indebted to Air Force Office of Scientific Research (AFOSR) for the financial support under grant No. FA9550-14-1-0279. D.F. and D.C. acknowledge support from National Science Foundation under the grant No. CMMI-1450806.